Enhanced Photoinduced Electron Transfer Through a Tyrosine Relay in a De Novo Designed Protein Scaffold Bearing a Photoredox Unit and a $Fe^{II}S_4$ Site

Alison Tebo,[a, b] Annamaria Quaranta,[c] Vincent L. Pecoraro,[b] and Ally Aukauloo*[c, d]

Electron transfer (ET) processes in biology over long distances often proceed via a series of hops, which reduces the distance dependence of the rate of ET. The protein matrix itself can be involved in mediating ET directly through the participation of redox-active amino acids. We have designed an electron transfer chain incorporated into a de novo protein scaffold, which is capable of photoinduced intramolecular electron transfer between a photoredox unit and a $Fe^{II}S_4$ site through a tyrosine amino acid relay. The kinetics were characterized by nanosecond laser pulse photolysis and revealed that electron transfer from $[Ru^{III}bpymal]^{3+}$ proceeds most efficiently via a tyrosine located ~16 Å from Rubpymal (bpymal = 1-((1-([2,2′-bipyridin]-4-yl)-1H-1,2,3-triazol-4-yl)methyl)-1H-pyrrole-2,5-dione). Removal of the tyrosine as the electron relay station results in a 20-fold decrease in the apparent rate constant for the electron transfer.

1. Introduction

Extending the degree of complexity of synthetic designed proteins can help expand the functional repertoire of highly sophisticated native systems in a minimalist replica. This quest may also lead chemists to the discovery of new ways to perform sustainable chemical transformations as biology has been doing for eons. The great leap in this field has been accomplished by the rational synthesis of targeted sequence peptides and their structural characterization. The incorporation of metal centers in designed coordinating pockets and the resulting catalytic performance has already demonstrated novel reactivity patterns.[1–3] Still, the integration of more sophisticated elements such as multiple functional sites, kinetic control of catalysis, and long-range communication between functional modules are the next challenges. Long distance electron transfer relays are functional aspects of many important protein systems involved in key steps of respiration, photosynthesis, and DNA synthesis.[4] Intermediate components that participate in long distance electron transfer chains include not only the classical metal-based and organic cofactors, but also amino acid side chains such as tyrosine[5–7] and tryptophan,[8,9] both of which are capable of single electron transfer reactions at high redox potential (~1 V *vs* NHE) that proceed via organic radicals.

Electron transfer relays have long been studied in proteins and protein assemblies such as Photosystem II (PSII) and ribonucleotide reductase (RNR) to understand these processes in their native context.[4] Synthetic chemists too have sought to incorporate relays into biomimetic molecular systems[10–17] as well as in catalytic systems.[18–22] While electron transfer has been examined by protein design,[23,24] the design of electron relays such as those found in PSII and RNR has been less studied. Not only does protein design offer the opportunity to examine the fundamental requirements for function in electron transfer relays, but the implementation of these principles into extant systems may provide new tools for improving the interfacing between grafted catalytic modules and the electrode or for providing directional electron transfer processes in artificial photosynthetic systems.

We have previously reported a designed peptide system capable of photo-triggered intramolecular electron transfer to generate a tyrosine radical.[25] In this system, a ruthenium (II) trisbipyridine derivative $[Ru^{II}bpymal]^{2+}$ (bpymal = 1-((1-([2,2′-bipyridin]-4-yl)-1H-1,2,3-triazol-4-yl)methyl)-1H-pyrrole-2,5-dione) is covalently attached to the surface of a designed peptide. An electron is transferred from the tyrosine to photogenerated ruthenium (III) in the presence of an external electron acceptor. This system displays pH dependent electron transfer typical of proton-coupled electron transfer (PCET) processes and has been characterized by nanosecond laser flash photolysis and electron paramagnetic resonance (EPR). We hypothesized that the tyrosine radical would be capable of electron transfer to another redox cofactor incorporated into the protein scaffold. We have recently reported an analogous three-helix bundle, α_3DIV-L21C, with a rubredoxin (FeS_4) site that is an excellent mimic for the spectroscopic features of

[a] *Dr. A. Tebo*
Program in Chemical Biology
University of Michigan
Ann Arbor (USA)
[b] *Dr. A. Tebo, Prof. V. L. Pecoraro*
Department of Chemistry
University of Michigan
Ann Arbor (USA)
[c] *Dr. A. Quaranta, Prof. A. Aukauloo*
Institut de Biologie Integrative de la cellule
CEA, Université Paris-Saclay
Gif-sur-Yvette (France)
E-mail: ally.aukauloo@universite-paris-saclay.fr
[d] *Prof. A. Aukauloo*
Institut de Chimie Moléculaire et des Matériaux d'Orsay
Université Paris-Saclay
Orsay (France)

Supporting information for this article is available on the WWW under https://doi.org/10.1002/cptc.202100014

© 2021 Wiley-VCH GmbH

rubredoxin.[26] This construct was then modified to include a C-terminal cysteine residue to which $[Ru^{II}bpymal]^{2+}$ was attached, now containing the three elements to interrogate the role of a redox active relay in a light triggered electron transfer process: a redox active tyrosine is intercalated between a photoactive ruthenium derivative and a tetrathiolate iron center (Figure 1). We report here, the results of transient absorption measurements in the presence of an external electron acceptor that demonstrate the participation of the tyrosine in the rapid conveyance of the hole transfer to the metallic center. We also found that the absence of the tyrosine in our model slows down the oxidation of the iron (II) center directly by the photoproduced oxidizing $[Ru^{III}bpymal]^{3+}$.

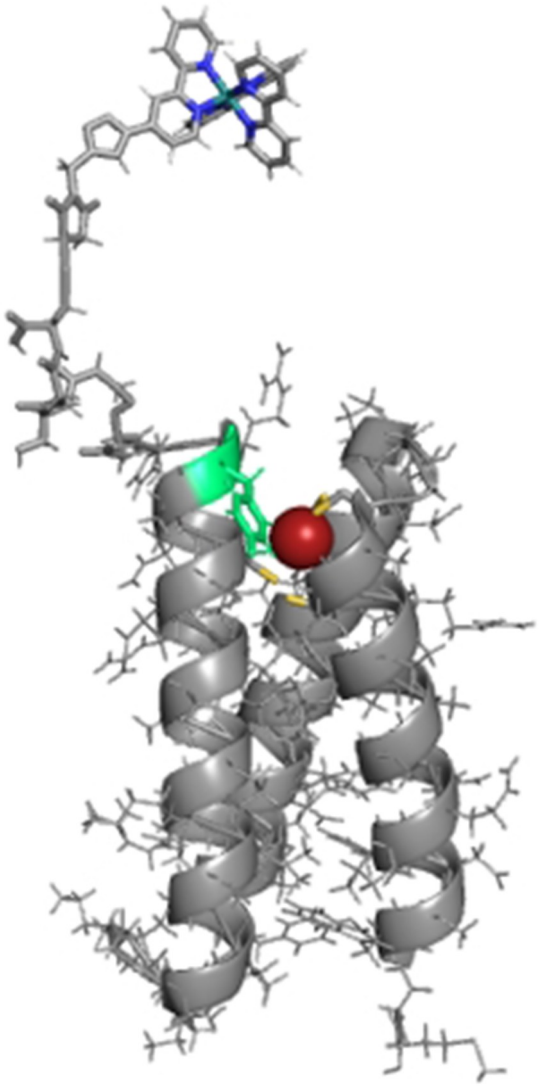

Figure 1. Schematic representation of the structure of α_3DIV-L21C-Rubpymal based on the solution structure of a closely related scaffold (PDB: 2MTQ). The red sphere represents the iron binding site and the green highlights the location of Tyr_{70}.

2. Results and Discussion

Prior to flash-quench experiments, we confirmed that the excited state of the sensitizer was not affected by the presence of the tetrathiolate iron center (Figure S1). We then characterized this construct, termed α_3DIV-L21C-$[Ru^{II}bpymal]^{2+}$, using nanosecond laser flash photolysis techniques in the presence of an external electron acceptor, methyl viologen, MV^{2+}. While previous studies have used the acceptor ruthenium hexamine, $[Ru^{III}(NH_3)_6]^{3+}$, as a reversible electron acceptor devoid of absorbing features in the visible region, we observed that $[Ru^{III}(NH_3)_6]^{3+}$ was capable of direct interaction with the FeS_4 site as evidenced by the formation of a colored complex pre-excitation. Excitation of $[Ru^{II}bpymal]^{2+}$ in the MLCT band at around 450 nm in the presence of MV^{2+} as a reversible electron acceptor resulted in the formation of the charge-separated state, $[Ru^{III}bpymal]^{3+}$ and $MV^{+\bullet}$. The highly oxidizing $[Ru^{III}bpymal]^{3+}$ ($E_{1/2} = 1.26$ V *vs* NHE)[27] can then react to rip an electron from Tyr_{70} ($E_{1/2} \sim 0.9$ V *vs* NHE),[28] which, in turn, is reset to its initial state by abstracting an electron from the $Fe^{II}S_4$ site ($E_{1/2} = -0.075$ V *vs* NHE).[26] Kinetic traces collected at wavelengths of interest were used to track the photophysical events of this sequential electron transfer reaction. Immediately post-laser flash, the system is characterized by a depletion of the MLCT signal with a minimum at 450 nm and a positive absorption with a maximum at 605 nm, which are indicative of the formation of Ru^{III} and $MV^{+\bullet}$, respectively. The disappearance of $[Ru^{III}bpymal]^{3+}$ at 450 nm, faster than the $MV^{+\bullet}$ decay at 605 nm, is accompanied by the growth of a positive signal at 410, 420, and 500 nm (Figure 2), indicated the presence of a subsequent process regenerating the Ru^{II}. The oxidized iron center is characterized by a broad series of LMCTs between 300 and 600 nm with maxima at 350 nm and 490 nm with $\varepsilon \sim 5000$ and 2700 $M^{-1}cm^{-1}$, respectively. This absorption overlaps with the intense bands of reduced methyl viologen ($\varepsilon = 39000\ M^{-1}cm^{-1}$ at 400 nm and $13000\ M^{-1}cm^{-1}$ at 605 nm)[26] making it difficult to clearly isolate the signals for the oxidized Fe^{III} species. A global fit of the kinetic traces at different wavelengths with a bi-exponential decay model results in an apparent rate constant associated with the positive absorption at 410/420 nm and 500 nm ($k_{app} = 1.4 \times 10^5\ s^{-1}$) and an apparent decay $k_d = 8.7 \times 10^3\ s^{-1}$. A single rate is thus found for the tyrosine/FeS_4 oxidation, assigned to the rate-determining step.

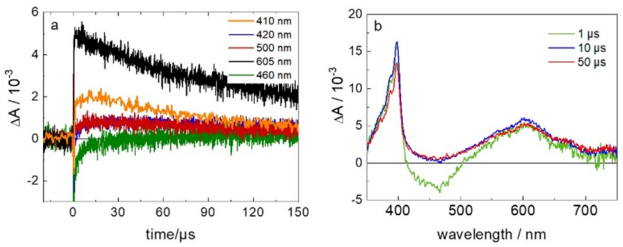

Figure 2. (a) Selected kinetics obtained for an aqueous solution containing α_3DIV-L21C-Rubpymal and 10 mM MV^{2+}. Excitation wavelength: 460 nm, laser energy = 10 mJ. (b) Differential absorption spectra obtained at different delays (in the legend) from laser pulse.

© 2021 Wiley-VCH GmbH

Indeed, given the close proximity between the iron site and the tyrosine side chain of ~5–7 Å, and the favorable driving force for Fe oxidation ($\Delta G \sim -1$ eV), it was not possible to distinguish the two kinetic steps.

We then performed control measurements to better characterize the peptide oxidation by Ru^{III}. Experiments carried out with the apo-protein display similar absorption features and kinetics for the tyrosine radical as was previously reported (Figure S2). In the presence of MV^{2+}, the tyrosyl radical appeared with an apparent rate $k_{app} = 1 \times 10^5\ s^{-1}$, followed by radical recombination with an apparent rate $k_d = 2 \times 10^4\ s^{-1}$. However, in the apo peptide the growth around 480 nm was not observed (Figure S3), suggesting that such signal in the α_3DIV-L21C-[Ru^{II}bpymal]$^{2+}$ originates from iron oxidation. The growth of absorption in this region occurs for the iron peptide at an apparent rate similar to the tyrosine oxidation rate in the apo peptide. This indicates that the tyrosine oxidation is indeed the rate-determining step in the α_3DIV-L21C-[Ru^{II}bpymal]$^{2+}$ peptide, and the subsequent iron oxidation by the tyrosine radical is faster.

As a further control, the iron-coordinated peptide lacking the C-terminal cysteine for [Ru^{II}bpymal]$^{2+}$ fixation, α_3DIV-L21C, was also characterized in a bimolecular reaction with [Ru^{II}-(bpy)$_3$]$^{2+}$ in solution (Figure S4). This is advantageous because it allows us to investigate the electron transfer reaction in a configuration where donor-acceptor distance and orientation are not fixed. Furthermore, the resulting reaction rate depends on the concentration of the reactants, which is an adjustable parameter. In the bimolecular reaction, in the presence of 100 μM of Fe-α_3DIV-L21C, the [Ru^{III}(bpy)$_3$]$^{3+}$ species probed at 450 nm disappears in a few μs (Figure S4) while the reduced $MV^{+\bullet}$ species is longer lived (Figure S4, blue trace). A bi-exponential decay global fit was used to obtain the apparent rate for [Ru^{II}(bpy)$_3$]$^{2+}$ recovery and the associated spectral changes. The resulting pseudo first order rate ($k_{bim} = 3.1 \times 10^9\ M^{-1}\ s^{-1}$) associated with the interaction of [Ru^{III}(bpy)$_3$]$^{3+}$ and the $Fe^{II}S_4$ containing peptide, is close to the diffusion limit, indicating that the rate-limiting step, in this case, is the formation of the encounter complex between [Ru^{III}(bpy)$_3$]$^{3+}$ and the Fe-coordinated peptide. The broad absorption obtained after the reduction of [Ru^{III}(bpy)$_3$]$^{3+}$ by the peptide suggests the generation of $Fe^{III}S_4$. Taken together, these results support our idea that the final electron donor within the peptide is $Fe^{II}S_4$.

To test the hypothesis that Tyr_{70} is capable of acting as a redox-active relay between [Ru^{II}bpymal]$^{2+}$ and the $Fe^{II}S_4$ site, we also characterized the electron transfer kinetics in a peptide in which all the tyrosine residues were mutated to phenylalanine, termed α_3DIV-L21C-YF-[Ru^{II}bpymal]$^{2+}$. The evolution of the spectrum, post-laser flash, suggests that an electron transfer event regenerates [Ru^{II}bpymal]$^{2+}$ from the charge separated state [Ru^{III}bpymal]$^{3+}$ while $MV^{+\bullet}$ still persists. In this case, oxidation should be located on Fe^{II}, since there are no other redox active amino acids that can be oxidized in the vicinity. Here again, a positive absorption signal is observed at wavelengths 400–500 nm, a feature characteristic of the oxidized $Fe^{III}S_4$ (Figure 3). A bi-exponential global fit of these data

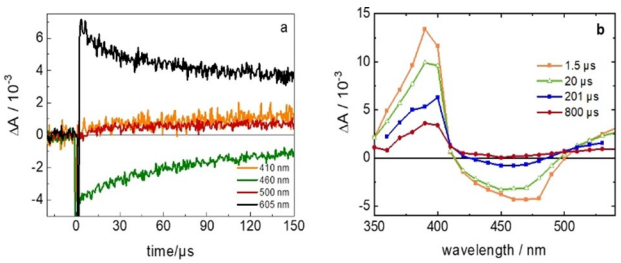

Figure 3. (a) Differential absorption kinetics for α_3DIV-L21C-YF-Rubpymal at kinetics of interest: 605 nm (maximum of $MV^{\bullet+}$), 460 nm (depletion of Ru^{II}) and at the growth of a new signal (410 nm, 500 nm). Excitation wavelength: 460 nm, laser energy = 10 mJ. (b) Differential absorption spectra obtained at different delays (in the legend) from laser pulse.

provides apparent rate constants $k_{app} = 6.3 \times 10^3\ s^{-1}$ and decay $k_d = 8 \times 10^2\ s^{-1}$. The slow rate for iron oxidation could also be compatible with an intermolecular reaction occurring between two different peptides. These results suggest a much slower iron oxidation in the absence of the tyrosine, and an oxidation that does not necessarily occur intramolecularly (Figure 4).

We have shown in this tripartite system that the removal of the intercalated tyrosine between the photoactive unit and the redox active metal center results in a decrease in the rate constant of electron transfer from Fe^{II} to Ru^{III} by about one order of magnitude. Our results support the involvement of the tyrosine in mediating electron transfer from Fe^{II} to Ru^{III}. This is consistent with our previous results characterizing a PCET process in a closely related peptide in which Tyr_{70} is able to reduce [Ru^{III}bypmal]$^{3+}$. The identity of the proton acceptor is not known but is likely to be a solvent molecule. Another possibility is a histidine residue two amino acids away, but which is facing towards the exterior of the α-helix and thus is not optimally positioned to accept a proton from Tyr_{70}. Based on the amplitude of the signal at 500 nm, assigned to the oxidized Fe^{III} form, the yield of Fe^{III} is ~25% smaller for α_3DIV-L21C-YF-[Ru^{II}bpymal]$^{2+}$ than for the tyrosine-containing peptide, α_3DIV-L21C-[Ru^{II}bpymal]$^{2+}$. This result elegantly points to the fact that the tyrosine is playing an efficient role as a relay in the electron transfer from $Fe^{II}S_4$ to [Ru^{III}bpymal]$^{3+}$.

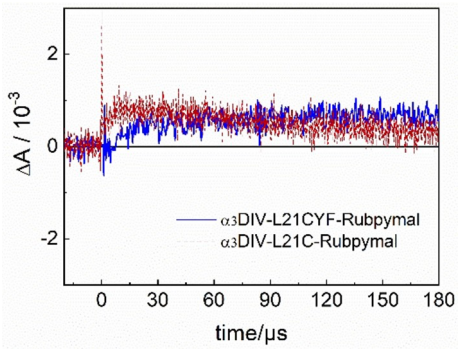

Figure 4. Differential absorption kinetics at 500 nm for the tyrosine-containing peptide (α_3DIV-L21C-Rubpymal) and the peptide lacking it (α_3DIV-L21C-YF-Rubpymal) in the presence of 10 mM MV^{2+}.

© 2021 Wiley-VCH GmbH

3. Conclusions

In summary, we have described an electron transfer chain incorporated into de novo designed protein scaffold, which is capable of photoinduced intramolecular electron transfer between two metal sites through an amino acid relay. This phenomenon has been observed in native proteins such as ribonucleotide reductase, where tyrosines are known to play key roles in facilitating long distance electron transfer to support physiologically relevant rates. The kinetics were characterized by nanosecond laser pulse photolysis and revealed that electron transfer from $Fe^{II}S_4$ to $[Ru^{III}bpymal]^{3+}$ proceeds most efficiently via a tyrosine located ~16 Å from Rubpymal. Electron transfer to the $[Ru^{III}bpymal]^{3+}$ proceeds with a k_{app} of $1.4\times10^5\ s^{-1}$, which is similar to the value we previously reported for a related peptide ($3.3\times10^5\ s^{-1}$).[25] Removal of the tyrosine results in a 20-fold decrease in the apparent rate constant for the electron transfer ($k_{app}=6.3\times10^3\ s^{-1}$). This designed system is a powerful tool to investigate the phenomenon of electron transfer relays in proteins. Further studies should focus on changing the elements of the relay to include other metal sites that have been characterized in this bundle such as copper, which could generate photocatalytic systems, as well as exchanging the tyrosine for a tryptophan, which also changes the driving force of the reaction. Furthermore, changing the position of the appended ruthenium would allow the determination of the distance dependence of intramolecular transfer and would allow us to tune the kinetics of electron transfer.

Acknowledgements

A.G.T. acknowledges training grant support from the University of Michigan Chemistry-Biology Interface (CBI) training program (NIH grant 5T32GM008597) as well as support from the Chateaubriand Fellowship. V.L.P would like to thank the National Institutes of Health (NIH) for financial support for this research (ES012236). This work has benefited from the facilities and expertise of the I2BC proteomic platform (Proteomic-Gif, SICaPS), supported by IBiSA, Ile de France Region, Plan Cancer, CNRS and Paris-Saclay University. This work was supported in part by the French Infrastructure for Integrated Structural Biology (FRISBI) ANR-10-INSB-05-01 and Labex CHARMMAT.

Conflict of Interest

The authors declare no conflict of interest.

Keywords: amino acids · electron relay · electron transfer · protein design · photoredox catalysis

[1] M. L. Zastrow, A. F. A. Peacock, J. A. Stuckey, V. L. Pecoraro, *Nat. Chem.* **2012**, *4*, 118–123.
[2] F. Yu, J. E. Penner-Hahn, V. L. Pecoraro, *J. Am. Chem. Soc.* **2013**, *135*, 18096–18107.
[3] K. J. Koebke, F. Yu, E. Salerno, C. Van Stappen, A. G. Tebo, J. E. Penner-Hahn, V. L. Pecoraro, *Angew. Chem. Int. Ed.* **2018**, *57*, 3954–3957; *Angew. Chem.* **2018**, *130*, 4018–4021.
[4] J. L. Dempsey, J. R. Winkler, H. B. Gray, *Chem. Rev.* **2010**, *110*, 7024–7039.
[5] J. J. Warren, J. R. Winkler, H. B. Gray, *FEBS Lett.* **2012**, *586*, 596–602.
[6] M. Cordes, A. Köttgen, C. Jasper, O. Jacques, H. Boudebous, B. Giese, *Angew. Chem. Int. Ed.* **2008**, *47*, 3461–3463; *Angew. Chem.* **2008**, *120*, 3511–3514.
[7] Q.-H. Dai, C. Tommos, E. J. Fuentes, M. R. A. Blomberg, P. L. Dutton, A. J. Wand, *J. Am. Chem. Soc.* **2002**, *124*, 10952–10953.
[8] B. A. Barry, *J. Photochem. Photobiol. B* **2011**, *104*, 60–71.
[9] B. A. Barry, *Nat. Chem.* **2014**, *6*, 376–377.
[10] M. T. Huynh, S. J. Mora, M. Villalba, M. E. Tejeda-Ferrari, P. A. Liddell, B. R. Cherry, A.-L. Teillout, C. W. Machan, C. P. Kubiak, D. Gust, T. A. Moore, S. Hammes-Schiffer, A. L. Moore, *ACS Cent. Sci.* **2017**, *3*, 372–380.
[11] J. D. Megiatto Jr, D. D. Méndez-Hernández, M. E. Tejeda-Ferrari, A.-L. Teillout, M. J. Llansola-Portolés, G. Kodis, O. G. Poluektov, T. Rajh, V. Mujica, T. L. Groy, D. Gust, T. A. Moore, A. L. Moore, *Nat. Chem.* **2014**, *6*, 423–428.
[12] G. F. Moore, M. Hambourger, M. Gervaldo, O. G. Poluektov, T. Rajh, D. Gust, T. A. Moore, A. L. Moore, *J. Am. Chem. Soc.* **2008**, *130*, 10466–10467.
[13] A. Magnuson, H. Berglund, P. Korall, L. Hammarström, B. Åkermark, S. Styring, L. Sun, *J. Am. Chem. Soc.* **1997**, *119*, 10720–10725.
[14] M. Sjödin, S. Styring, B. Åkermark, L. Sun, L. Hammarström, *J. Am. Chem. Soc.* **2000**, *122*, 3932–3936.
[15] M. Sjödin, R. Ghanem, T. Polivka, J. Pan, S. Styring, L. Sun, V. Sundström, L. Hammarström, *Phys. Chem. Chem. Phys.* **2004**, *6*, 4851–4858.
[16] O. S. Wenger, *Coord. Chem. Rev.* **2015**, *282–283*, 150–158.
[17] M. Natali, S. Campagna, F. Scandola, *Chem. Soc. Rev.* **2014**, *43*, 4005–4018.
[18] F. Lachaud, A. Quaranta, Y. Pellegrin, P. Dorlet, M.-F. Charlot, S. Un, W. Leibl, A. Aukauloo, *Angew. Chem. Int. Ed.* **2005**, *44*, 1536–1540; *Angew. Chem.* **2005**, *117*, 1560–1564.
[19] A. Baron, C. Herrero, A. Quaranta, M.-F. Charlot, W. Leibl, B. Vauzeilles, A. Aukauloo, *Inorg. Chem.* **2012**, *51*, 5985–5987.
[20] A. Baron, C. Herrero, A. Quaranta, M.-F. Charlot, W. Leibl, B. Vauzeilles, A. Aukauloo, *Chem. Commun.* **2011**, *47*, 11011–11013.
[21] C. Herrero, J. L. Hughes, A. Quaranta, N. Cox, A. W. Rutherford, W. Leibl, A. Aukauloo, *Chem. Commun.* **2010**, *46*, 7605–7607.
[22] C. E. Castillo, S. Romain, M. Retegan, J.-C. Leprêtre, J. Chauvin, C. Duboc, J. Fortage, A. Deronzier, M.-N. Collomb, *Eur. J. Inorg. Chem.* **2012**, *2012*, 5485–5499.
[23] C. C. Moser, P. L. Dutton, *Biochim. Biophys. Acta Bioenerg.* **1992**, *1101*, 171–176.
[24] B. R. Gibney, S. E. Mulholland, F. Rabanal, P. L. Dutton, *PNAS* **1996**, *93*, 15041–15046.
[25] A. G. Tebo, A. Quaranta, C. Herrero, V. L. Pecoraro, A. Aukauloo, *ChemPhotoChem* **2017**, *1*, 89–92.
[26] A. G. Tebo, T. B. J. Pinter, R. García-Serres, A. L. Speelman, C. Tard, O. Sénéque, G. Blondin, J.-M. Latour, J. Penner-Hahn, N. Lehnert, V. L. Pecoraro, *Biochemistry* **2018**, *57*, 2308–2316.
[27] K. Kalyanasundaram, *Coord. Chem. Rev.* **1982**, *46*, 159–244.
[28] S. D. Glover, R. Tyburski, L. Liang, C. Tommos, L. Hammarström, *J. Am. Chem. Soc.* **2018**, *140*, 185–192.

Manuscript received: January 19, 2021
Revised manuscript received: February 22, 2021
Accepted manuscript online: March 15, 2021
Version of record online: April 8, 2021

© 2021 Wiley-VCH GmbH